Acta Botanica Brasilica, 2024, 38: e20230226
doi: https://doi.org/10.1590/1677-941X-ABB-2023-0226

Original Article

Anthocyanin Accumulation and Chlorophyll Degradation Lead to the Formation of Colourful Leaves of *Syringa oblata* in Autumn

Meiling Han[1], Rui Lu[1], Meng Han[1], Xiuyun Yang[2], Fang Du[1], Xiaoping Chen[1,*], Saiwei Huang[1], Shan Luo[1] and Dongliang Han[1]

[1]Shanxi Agricultural University, College of Urban and Rural Construction, Taigu, China
[2]Shanxi Agricultural University, College of Forestry, Taigu, China
*Corresponding author: cxp198905@hotmail.com

ABSTRACT

Syringa oblata is an important garden plant whose leaf colour turns from green to red in autumn when air temperature and daylength decrease. This study explored the reasons for leaf reddening by detecting phenotypic characteristics and pigment types and contents. With leaf reddening, luminance L^* increased and chrominance a^* decreased significantly. Chlorophyll and carotenoid contents significantly decreased in accordance with the distribution change of green pigment in leaf cells. Conversely, the red pigment distribution increased and the total polyphenol, total flavonoid and total anthocyanin contents evidently increased. Anthocyanin accumulation was the important reason for leaf reddening. Of the anthocyanins detected in leaves, cyanidin and delphinidin-3-*O*-rutinoside contents gradually increased with leaf reddening and were negatively correlated with L^*. They were considered key anthocyanins influencing leaf colour. Apigenin and syringic acid were correlated with delphinidin-3-*O*-rutinoside and cyanidin, and they could be the anthocyanin co-pigments. Cyanidin-3-*O*-arabinoside and taxifolin were more abundant polyphenols in leaves. In summary, anthocyanin accumulation and chlorophyll degradation occurred along with leaf reddening. Temperature, light, and other co-pigments influenced the anthocyanin and chlorophyll contents. This study provides evidence for applications of *S. oblata* as a coloured-leaf plant in gardens and as a source of active ingredients in the commercial market.

Keywords: *Syringa oblata*, colour-leaf plant, leaf colouration, anthocyanin, chlorophyll, polyphenol

Introduction

Syringa oblata Lindl., belonging to the family Oleaceae, is widely cultivated as an ecological and ornamental tree, spanning subtropical, warm temperate, temperate and the edge of cold temperate zones (Ma *et al.* 2022). The major ornamental traits of *S. oblata* depend on its flowers, which are bright blue-purple in colour and have a fine fragrance in spring. The leaves of *S. oblata* change colour from green to red in autumn, suggesting that *S. oblata* is a coloured-leaf plant. The diversity of colouration patterns during autumn senescence has important ecological significance (Feild *et al.* 2001), however, few studies have reported on *S. oblata* leaf colour.

Received July 30, 2023; Accepted December 15, 2023
Editor-in-Chief: Thaís Elias Almeida; Associate Editor: Bruno Garcia Ferreira

How to cite:
Han M, Lu R, Han M *et al.* 2024. Anthocyanin Accumulation and Chlorophyll Degradation Lead to the Formation of Colourful Leaves of *Syringa* oblata in Autumn. Acta Botanica Brasilica 38: e20230226. doi: 10.1590/1677-941X-ABB-2023-0226

Anthocyanins, chlorophylls, and carotenoids are the main pigments in plant leaves, and their contents and distributions determine leaf colour (Tang *et al*. 2020; Li W *et al*. 2022). Chlorophylls, mainly chlorophylls a and b in higher plants, are the key photosynthetic pigments making leaves green (Shi *et al*. 2021). Carotenoids help to protect the photosynthetic apparatus from photo-oxidation and make plants appear yellow, orange, or red (Shen *et al*. 2019; Liu *et al*. 2021). Anthocyanins are phenolic compounds and their different types confer the red, orange, purple, and yellow colour to plant leaves (Khusnutdinov *et al*. 2021). Anthocyanin accumulation and chlorophyll degradation contribute to the leaf colouration of *Quercus dentata* during autumn (Wang *et al*. 2023). Environmental factors also affect leaf colour by influencing anthocyanin and chlorophyll metabolism (Xu *et al*. 2015; Lu *et al*. 2016; Song *et al*. 2019; Lee *et al*. 2023).

Some studies have reported on pigment substances of the genus *Syringa*. Zhang *et al*. (2022) found that phenylpropanoids are phylogenetically conserved in *Syringa* plants, enhancing their ability to adapt to the environment. Additionally, leaves from *S. oblata* var. *alba*. were found to contain high levels of total polyphenol (Nenadis *et al*. 2007). Sun and Guo (2013) studied the extraction process of total flavonoid from *S. oblata*. Total flavonoid contents of *S. wolfii* branches at different harvest stages were significantly different (Han *et al*. 2011). Notably, during the spring leaf-expansion stage of *S. oblata*, the quantity of anthocyanin decreased while that of chlorophyll increased (Tian *et al*. 2014). While flavonoids, including kaempferol-3-*O*-α-*L*-rhamnosyl-β-*D*-glucoside, quercetin, rutin, quercetin-3-*O*-β-*D*-glucoside, and naringenin, have been identified in *S. oblata* leaves (Tai *et al*. 2022), the specific types of anthocyanin remain unclear at present.

Some trees, such as *Liquidambar formosana*, *Populus deltoides*, *Ginkgo Biloba,* and *Acer pseudosieboldianum*, have been examined only as foliage plants to explore the leaf colouring mechanism in autumn (Wen *et al*. 2015; Li *et al*. 2018; Zhang *et al*. 2019; Li X *et al*. 2022). *S. oblata* is an important flower plant in spring, and its leaves turn red with the cool temperatures in autumn, which prolongs its ornamental periods. Therefore, exploring the leaf reddening mechanism in *S. oblata* in autumn will provide the theoretical basis for similar leaf colour change in other species of plants during autumn.

This research aims to explore the reason for leaf reddening in *S. oblata* by analyzing the relationships among phenotypic characteristics, environmental factors, and pigment contents, as well as determining the key anthocyanins influencing leaf colour change. Thus, *S. oblata* leaves at seven stages were collected in autumn and had their phenotypic characteristics evaluated and the contents of total polyphenol, total flavonoid, total anthocyanin, chlorophyll, and carotenoid determined. Phenolic content and composition were also analyzed. These data were then used to evaluate our hypothesis that: (1) the content and proportional changes of chlorophyll, anthocyanin and carotenoid influence the leaf colour of *S. oblata*; (2) there may be one or several anthocyanins whose contents significantly correlate with the change in leaf phenotype; (3) and chlorophyll degradation and anthocyanin accumulation should be related to changes in air temperature, light, and some phenolic compounds during leaf senescence process.

Materials and methods

Plant materials and environment factors

Syringa oblata Lindl. leaves were collected in October 2022, at Shanxi Agricultural University, Taigu, Shanxi, China (37°43'N, 112°59'E). The study objects comprised three sturdy and eight-year-old trees. *S. oblata* leaves were divided into seven stages according to colour changes by observation, namely Stage 1 (S1), leaf is all-green; S2, central vein of leaves presents light red locally; S3, 50%–75% of leaf surface changes orange-red; S4, most of leaf surface is red; S5, leaf completely turn red; S6, leaf colour further deepens to purple-red hue and leaf thickness increases; S7, leaf shows a purplish reddish hue, and leaf is about to fall. At least ten intact leaves in the different parts of the trees at each stage were picked. A part of leaves was cut into diamond-shaped pieces, weighted at 0.1 g, and then frozen at -20 °C for subsequent experiments.

Daylength data were obtained from a website (https://sunrise.supfree.net/), and air temperature data were obtained from China Meteorological Data Network (http://data.cma.cn).

Colour values, pigment distribution in cells, and leaf pH determination

Pictures of *S. oblata* leaves at different stages were photographed by cellphone camera in the same indoor environment. The camera parameters were photo-sensibility 800 in the white balance model. The colour parameters of the pictures were captured by Adobe Photoshop 2021, and L^*, a^*, b^*, H^* and S^* values were recorded. Luminance (L^*) ranges from 0 to 100 where 0 is black and 100 is white. Hue angle (H^*) and saturation (S^*) were also taken into account. Chrominance a^* reflects the amount of redness (positive) to greenness (negative), while chrominance b^* indicates the amount of blueness (negative) to yellowness (positive). The colour bars were generated by paint bucket tool of Adobe Photoshop 2021 using the aforementioned colour pararmeters.

Fresh leaves of *S. oblata* were washed and soaked in distilled water to moisten and set aside. The tissue was cut parallel along the cut of leaf with a double-sided blade. Subsequently, the slide was gently removed by a glass slide. It was observed and photographed pictures for recording

under the optical microscope (Olympus, CX33RTFS2). The magnification was 40 × 10 times.

First, 0.1 grams of fresh leaves were ground with a little liquid nitrogen. Then 5 mL of deionized water was added to form a solution. Leaf pH was determined by a thunder magnetic portable multi-parameter magnetometer (DZB-712F).

Pigment extraction

Fresh leaves were divided into 0.1 g aliquot and ground into a powder with liquid nitrogen. Then, 5.0 mL of methanol solution was added and left in the dark for 48 h at 4 °C for phenolic extraction. 0.1 g fresh leaves were ground into powder with liquid nitrogen, and 10 mL 96% ethanol was added. The mixture was stored at 4 °C in the dark for 30 h for chlorophyll and carotenoid extraction. During this time, the mixture was shaken and blended every 8 h to ensure adequate pigment extraction. After that, the extract was then centrifuged at 4000 rpm at 4 °C for 10 min, and the supernatant was collected and transferred to 15.0 mL centrifuge tube and stored at 4 °C for analysis.

Chlorophyll and carotenoid content determination

Ethanol extract with a 2.0 mL volume was used to determine the absorbance at the wavelengths of 470 nm, 645 nm, and 663 nm. 96% ethanol was used as the blank control. The chlorophyll and carotenoid contents were determined using reported methods (Walibai *et al*. 2017). The calculation formulas are as follows:

C_a=13.95D_{663} – 6.88D_{645} (1)

C_b=24.96D_{645} – 7.32D_{663} (2)

C_{a+b}=C_a+C_b=6.63D_{663} + 18.08D_{645} (3)

C_x=(1000D_{470} – 2.05C_a – 114C_b)/245 (4)

Chloroplast content (mg·g^{-1} FW)=C*V*/M/1000 (5)

(Note: D_{470}, D_{645} and D_{660} are the absorbance of ethanol extract at 470 nm, 645 nm and 663 nm, respectively; C_a, C_b, C_{a+b}, and C_x are respectively the concentrations of chlorophyll a, chlorophyll b, total chlorophyll and carotenoid (mg·L^{-1}); V is the constant volume of chloroplast pigment extract (mL), M is the weight of the sample (g).).

Polyphenol content determination

The total polyphenol content was determined by the Folin-Ciocalteu reagent method (Wolfe *et al*. 2003) with some modifications. Specifically, 0.5 mL sterilized primary water and 0.125 mL extract were added into a 10 mL centrifuge tube, and then 0.125 mL Folin-Ciocalteu reagent was added. After mixing the solution well and reacting at room temperature for 6 min, 1.25 mL 7% Na_2CO_3 solution and 3.0 mL sterilized primary water were added to the above mixture, which was mixed well and reacted again at room temperature for 90 min away from light. The absorbance of the mixture at 760 nm was measured and recorded. Meanwhile, the standard curve was made using gallic acid and the results were represented as (mg GAE·g^{-1} FW).

The total flavonoid content was determined by aluminum chloride (Li *et al*. 2014). First, 1.25 mL sterilized primary water and 0.125 mL extract were added into a 10 mL centrifuge tube, followed by 0.075 mL 5% $NaNO_2$ solution and 0.15 mL 10% $AlCl_3$ solution, which were thoroughly mixed and reacted at room temperature for 6 min. Subsequently, 0.5 mL of NaOH solution (1 M) and 0.275 mL of sterilized primary water were added. Finally, the absorbance of the reaction solution at 510 nm was measured and recorded. Meanwhile, rutin solution was used to make the standard curve and the unit of calculation was (mg RE·g^{-1} FW).

The total anthocyanin content was determined by the methanol-HCl method (Li *et al*. 2012) with minor modifications. 1.6 mL of extract solution was taken and added with 25.0 μL HCl (12 mmol·L^{-1}). The reaction solution was mixed and then reacted at room temperature for 15 min away from light. Finally, the absorption values of the reaction solution at 530 nm, 620 nm and 650 nm were measured by ultraviolet spectrophotometer and recorded. The standard curve was made using cyanidin-3-*O*-glucoside and the results were represented as (mg CGE·g^{-1} FW).

The calculation formulas of polyphenol contents are as follows:

C_p = 0.4144*OD_{760} + 0.0358, R^2 =0.9999 (1)

C_f = 2.7888*OD_{510} – 0.1861, R^2 = 0.9999 (2)

OD_a = (OD_{530} – OD_{620})-0.1*(OD_{650} – OD_{620}) (3)

C_a = 0.0345*OD_a – 0.0028, R^2 = 0.9992 (4)

The content =C*V*/M (5)

(Note: D_{760}, OD_{510}, OD_{530}, OD_{620}, OD_{650} is the absorbance at 760, 510, 530, 620, and 650 nm, respectively. OD_a is the anthocyanin absorbance calculated by removing chloroplast absorbance. C, namely, C_p, C_f, or C_a, is the concentrations of the total polyphenol, total flavonoid, total anthocyanin (mg·mL^{-1}), respectively; V is the constant volume of pigment extract (mL), M is the weight of the sample (g).)

Analysis of phenolic metabolites

High Performance Liquid Chromatography coupled with a diode array detector (HPLC-DAD) was utilized to examine the types and quantities of phenolic metabolites within *S. oblata* leaves. The above-mentioned methanol extract was filtered through a 0.45 μm filter. HPLC-DAD analysis was performed using an LC-2030C Liquid Chromatograph (Shimadzu, Kyoto, Japan) equipped with an Inertsil C-18 column (5.0 μm particle size, 4.6 mm inner diameter × 250 mm length). HPLC-DAD separation was conducted by using a linear gradient of A (0.04% formic acid dissolved in water) and B (100% acetonitrile) solutions at 40 °C with a flow rate of 0.5 mL·min^{-1}. The solvent gradient used was as follows: 0 min, 5% B; 40 min, 40% B; 45 min, 100% B; then hold for 15 min. The post-run time was 10 min, as previously described by Han *et al*. (2022). The phenolic compounds

were determined by comparing their retention times and UV spectral data with those of the known standards. The phenolic metabolite contents were calculated using the corresponding standard calibration curves (Table S1).

Statistical analysis

Three biological replicates and three technical replicates were performed for all experiments, and the results were expressed as mean ± standard deviation (SD). IBM SPSS Statistics 26 was used to perform a One-Way Analysis of Variance (ANOVA). Origin 2021 was used to conduct the correlation analysis including Pearson's correlation analysis and principal component analysis (PCA). Office Excel 2016 was used to perform basic data analysis.

Results

Phenotypic characteristic changes in *S. oblata* leaves

The phenotypic changes of *S. oblata* leaves were observed in October 2022, when the air temperature declined and the daylength was shortened (Fig. 1A). From S1 to S7, there was a change in leaf colour from green to purple-red, as depicted in Fig. 1B. Specifically, the leaves were all green at S1, turned red from S2, and changed to all red at S5. After, the leaf colour was deepened and the leaf hardness was enhanced, showing features of leaf senescence (Fig. 2B). The abaxial leaf surface was green at all times (Fig. 2D).

The colour values of leaves were captured, and colour bars were plotted by software (Fig. 2A). Colour bars changed from green to purple-red from S1 to S7, which was consistent with the observed change in leaf colour. It is noteworthy that L^* and b^* values gradually decreased from 65 to 44 and from 44 to -1, respectively, whereas a^* values increased from -25 to 31 during leaf colouration (Table 1). The leaf pH was stable from 6.06 to 6.60 during leaf senescence (Table 1).

Pigment distributions in leaf cells were observed under a microscope (Fig. 2C). Pigments mainly accumulated in the cells of upper epidermal and palisade tissue cells. At S1, chlorophyll was observed in palisade tissue and spongy tissue cells. Anthocyanin appeared in the palisade tissue cells at S2 when chlorophyll degradation was evident, and accumulated the most at S5. Besides palisade tissue cells, the anthocyanin was distributed in the upper epidermal cells from S5 to S7. However, the red colour of palisade tissue cells faded visibly at S6 and S7. Spongy tissue cells were green all the time and the lower epidermal cells showed no colour, which was consistent with leaf phenotypes.

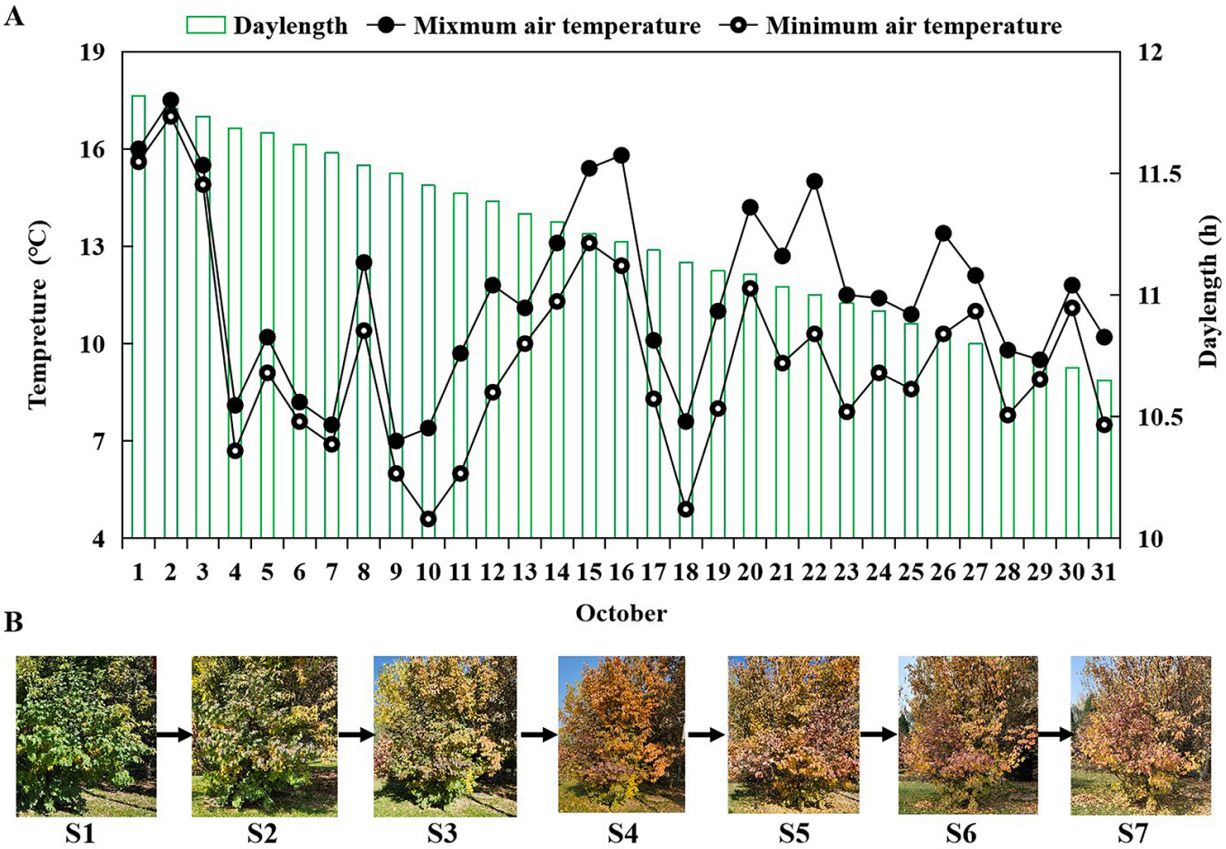

Figure 1. The changes in environment factors and tree forms of *Syringa oblata*. (A) The daylength and air temperature in October in the study area. (B) The tree forms of *Syringa oblata* at different senescence stages.

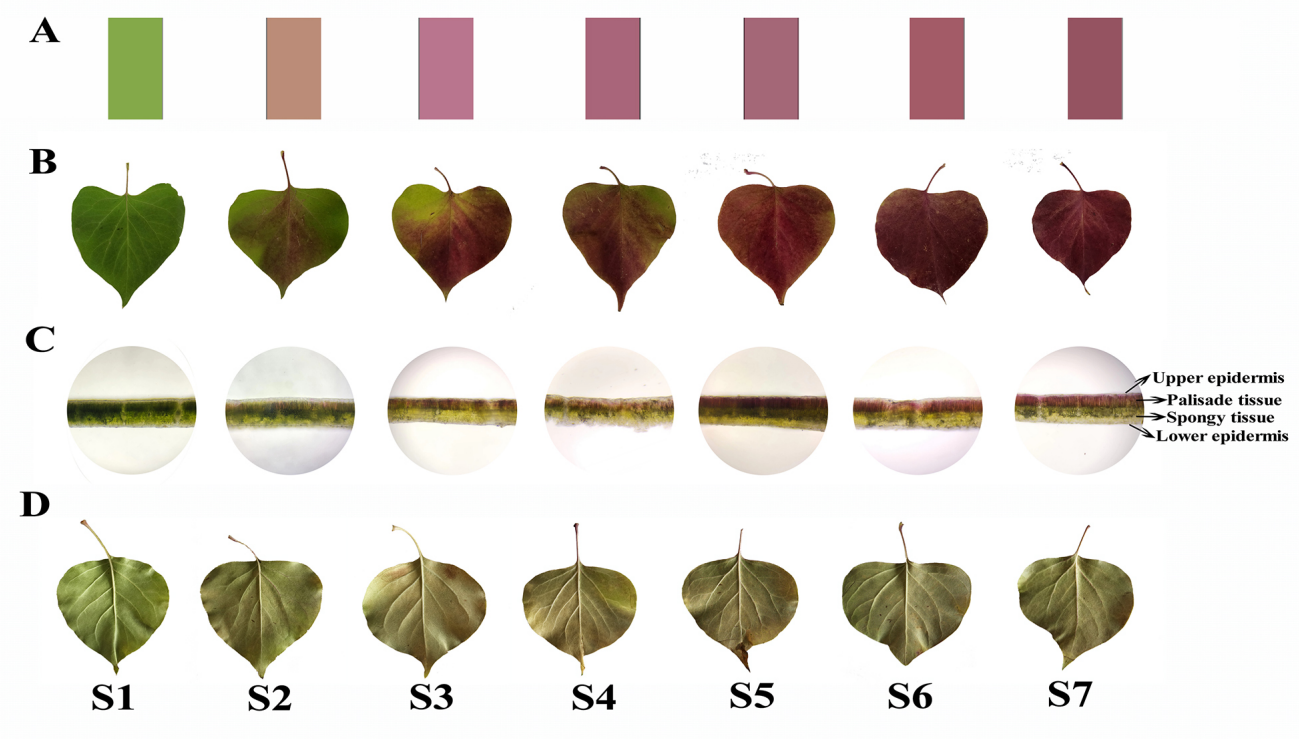

Figure 2. The phenotypic characteristics of *Syringa oblata* leaves at different senescence stages. (A) The colour bars obtained from leaf pictures by Adobe Photoshop 2021. (B) The colour change process of upper leaf surface from S1 to S7. (C) The pigment distributions in leaf cell, and the magnification is 40 × 10 times. (D) The colour change process of lower leaf surface from S1 to S7.

Table 1. The colour values and cell pH of *Syringa oblata* leaves.

Stage	L*	a*	b*	H*	S*	pH
S1	65	-25	44	83	57	6.60±0.12
S2	62	16	19	19	36	6.37±0.08
S3	57	30	-1	339	37	6.22±0.05
S4	51	30	1	342	40	6.19±0.03
S5	51	27	1	343	37	6.09±0.04
S6	48	31	7	350	44	6.06±0.03
S7	44	29	5	347	44	6.17±0.04

Chlorophyll and carotenoid contents of *S. oblata* leaves

The contents of chlorophyll a and b decreased gradually with leaf reddening in autumn. Consistently, the total chlorophyll contents dropped from the maximum value of 0.88 mg·g^{-1} FW at S1 to the minimum value of 0.07 mg·g^{-1} FW at S7 (Fig. 3A). Thus, the decline of the chlorophyll content was the major reason for the loss of green colour during leaf senescence.

Similarly, the carotenoid contents gradually decreased from S1 to S7, with a maximum value of 0.23 mg·g^{-1} FW to the minimum value of 0.024 mg·g^{-1} FW (Fig. 3B).

Polyphenol contents of *S. oblata* leaves

The total polyphenol and total flavonoid contents in *S. oblata* leaves were maintained at a high-level during leaf senescence (Fig. 3CD). Specifically, the total polyphenol contents first increased from S1 to S5 and then declined after S5. The highest content of 29.75 mg GAE·g^{-1} FW was found at S5, and the lowest content of 19.62 mg GAE·g^{-1} FW was detected at S1 (Fig. 3C). The total flavonoid content of leaves was unstable from S1 to S3 and declined gradually from S4 to S7. The highest level was detected at S4, reaching the value of 112.33 mg RE·g^{-1} FW (Fig. 3D).

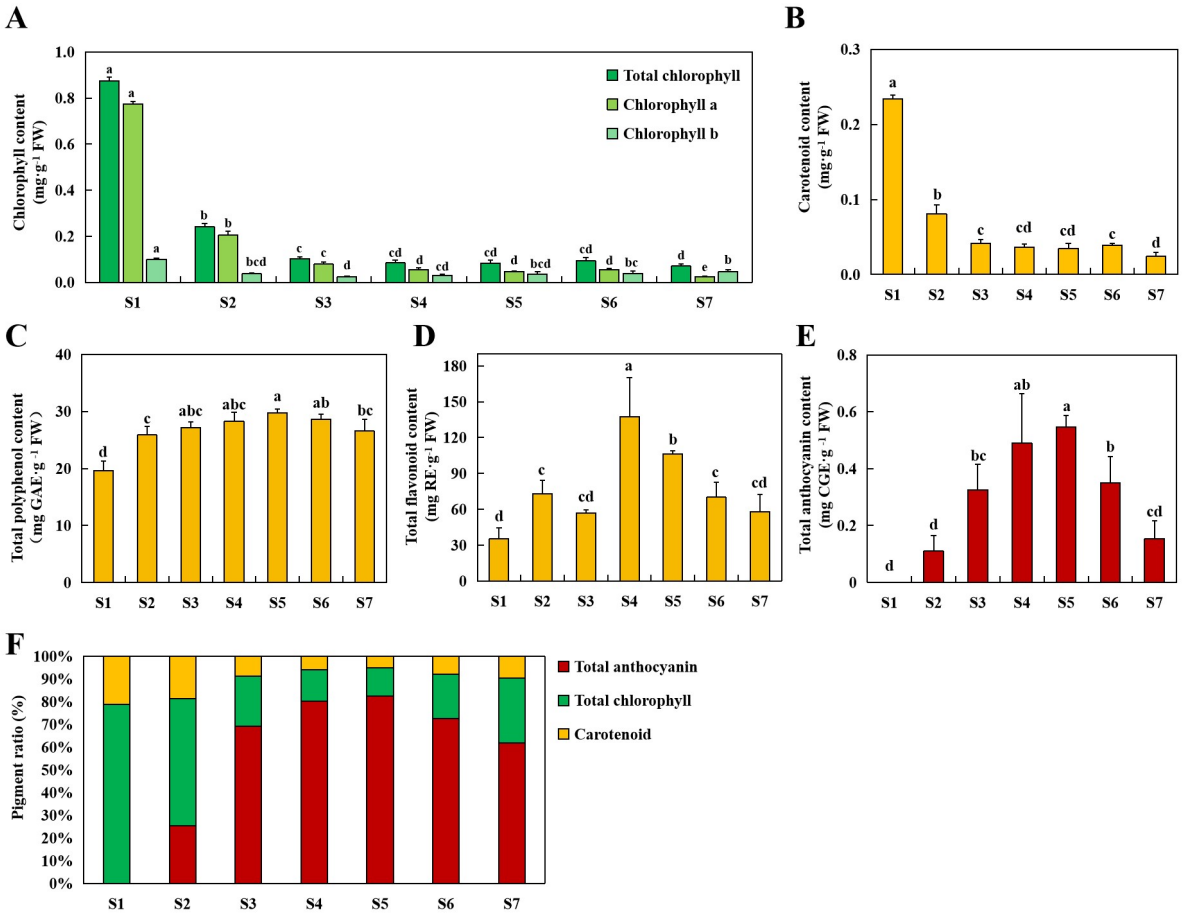

Figure 3. The change trends of pigment contents in *Syringa oblata* leaves. (A) Total chlorophyll, chlorophyll a and b contents. (B) Carotenoid contents. (C) Total polyphenol contents. (D) Total flavonoid contents. (E) Total anthocyanin contents. All values are the mean±SE, and different letters represent significant differences ($P < 0.05$) at different senescence stages. (E) Pigment ratios of total anthocyanin, total chlorophyll, and carotenoid in leaves.

Total anthocyanin contents changed significantly during leaf senescence (Fig. 3E), evidently increasing from S2 to S5 (with the highest content of 0.55 mg CGE·g^{-1} FW), and falling at S6 and S7. These changes were in keeping with the pigment distribution pattern in leaf cells. Thus, anthocyanin accumulation might be the main factor accelerating leaf reddening.

Further, analysis of the ratios of different pigments in leaves (Fig. 3F) found that total chlorophyll content had the highest proportion in leaves at S1 and S2. However, total anthocyanin rapidly achieved the highest proportion from S3 to S7. Carotenoid ratios were the lowest compared with chlorophyll and anthocyanin ratios, indicating that this pigment might not contribute to the leaf colouration.

Phenolic metabolites of *S. oblata* leaves

Twelve phenolic metabolites in *S. oblata* leaves were detected by HPLC-DAD, including four anthocyanins and other polyphenols (Fig. 4A).

The anthocyanins detected in leaves included cyanidin-3-*O*-arabinoside, cyanidin-3-*O*-rutinoside, delphinidin-3-*O*-rutinoside, and cyanidin (Fig. 4AB). Notably, delphinidin-3-*O*-rutinoside and cyanidin contents increased significantly during leaf reddening, with their highest values of 0.99 and 0.75 mg·g^{-1} FW, respectively, being at S7. Cyanidin-3-*O*-arabinoside was the most abundant polyphenol detected in *S. oblata* leaves, and its contents gradually decreased from S1 to S7. Cyanidin-3-*O*-rutinoside content remained constant from S1 to S7. As a result, the changes in cyanidin and delphinidin-3-*O*-rutinoside contents were highly correlated with the phenotypic changes in leaf colour.

Besides anthocyanins, other phenolic compounds were detected in *S. oblata* leaves, including taxifolin, isorhamnetin, apigenin, paeonol, resveratrol, syringic acid, *p*-coumaric acid, and salicylic acid (Fig. 4A). Among these polyphenols, taxifolin remained at high and stable levels during leaf senescence. Apigenin content increased evidently with leaf reddening, from 0.27 to 1.28 mg·g^{-1} FW. Similarly, syringic acid content was observed to increase from S1 to S7, particularly at S5 and S7. Isorhamnetin, paeonol, *p*-coumaric acid, resveratrol, and salicylic acid maintained stable and low levels in leaves at all times.

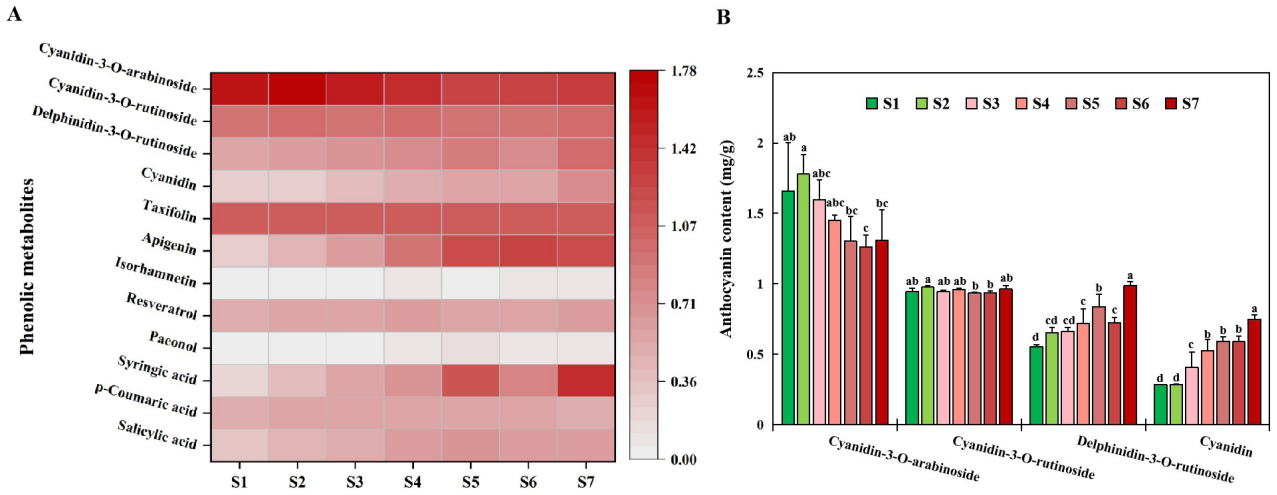

Figure 4. The phenolic metabolites in *Syringa oblata* leaves. (A) The kinds and contents of phenolic metabolites. Different red colours represent compound contents, the darker the red explains the higher the content. (B) The contents of four anthocyanins. Values are the mean±SE, and different letters represent significant differences ($P < 0.05$) at different senescence stages.

Correlation analysis

Pearson's correlation analysis was performed to reveal the relationships among pigments and colour parameters (Fig. 5). Values for L^* and b^* were negatively related to most of the phenolic compounds, such as delphinidin-3-*O*-rutinoside and cyanidin, but significantly and positively correlated with the total chlorophyll and carotenoid contents. In contrast, significant and negative correlations were found between a^* values and chlorophyll and carotenoid contents, but positive correlations with the contents of total polyphenol, total anthocyanin, isorhamnetin, resveratrol, and salicylic acid. Besides, delphinidin-3-*O*-rutinoside and cyanidin were significantly and evidently correlated with apigenin, paeonol, syringic acid and salicylic acid.

A PCA model was established to evaluate pigment contributions to leaf colouration (Fig. 6; Table 2). Principal components (PCs) 1, 2, and 3 explained 64.73%, 17.11%, and 8.76% of the total variance, respectively, which contained most statistical data analyzed and could be utilized to comprehensively evaluate the pigment contents of *S. oblata* leaves. In PC1, the loading plots of a^*, H^*, total polyphenol, total flavonoid, total anthocyanin, delphinidin-3-*O*-rutinoside, cyanidin, apigenin, isorhamnetin, paeonol, syringic acid, resveratrol, and salicylic acid were all positive and more than one. In contrast, the loading plots of L^*, b^*, S^*, total chlorophyll, carotenoid, and cyanidin-3-*O*-arabinoside were negative and more than one. These two groups were distributed on the left and right of the X-axis, respectively, indicating counterinfluence on leaf colouration. Consistently, the coefficients between PC1 and these indicators identified this result. In addition, PC2 was positively correlated with S^*, taxifolin, and *p*-coumaric acid. Thus, the PCA results were similar to those of Pearson's correlation analysis.

Discussion

The leaves of many plants change from green to yellow or red in autumn, which plays an increasingly important role in response to changes in the external environment and ornamental application. The contents and proportions of anthocyanins, chlorophylls, and carotenoids can influence leaf colour (Li W *et al*. 2022). Carotenoid contents accounted for a lower proportion in *S. oblata* leaves, and dropped during the leaf reddening process, indicating that carotenoid was not a major pigment for leaf reddening. Some yellow and orange autumn leaves were caused by carotenoid pigments unmasked by chlorophyll breakdown, but carotenoid concentrations steadily declined in both yellow- and red-senescing leaves, being replaced by the accumulation of anthocyanins (Lee *et al*. 2003; Nakashima & Yamakita 2023).

A visible sign of leaf senescence is the de-greening caused by rapid chlorophyll degradation during chloroplast degeneration, and this process is often accompanied by the accumulation of anthocyanin pigments in the vacuole (Feild *et al*. 2001; Gao *et al*. 2016; Sui *et al*. 2017; Renner & Zohner 2019). Leaf colour of *S. oblata* changed significantly from green to red in autumn. The chlorophyll distribution gradually diminished, and anthocyanin distribution evidently increased in leaf cells from S1 to S7. Concurrently, the chlorophyll contents gradually decreased. In contrast, the contents of total polyphenol, total flavonoid, and total

anthocyanin increased significantly with leaf reddening. The changes of the total anthocyanin contents were consistent with the phenotypic characteristic, colour value a*, and red pigment distribution in leaf cells. The analysis of pigment proportions explained the roles of chlorophyll and anthocyanin during leaf reddening. Thus, the leaf reddening in *S. oblata* in autumn is largely determined by the combined effects of chlorophyll degradation and anthocyanin accumulation. Similar results were found in the senescent leaves of *Pistacia chensisin* and *Acer pictum* subsp. *mono* (Song *et al*. 2021; Lin *et al*. 2023).

In the temperate zone, decreasing day length and cooler temperatures induce the breakdown of leaf chlorophyll during senescence (Sui *et al*. 2017; Renner & Zohner 2019) and low temperature induces anthocyanin biosynthesis (Gazula *et al*. 2005). The air temperature decreased in October in the study area, which could induce chlorophyll degradation and anthocyanin accumulation during leaf senescence process of *S. oblata*. Though the content changes of chlorophyll and anthocyanin are in the opposite direction, some reports revealed that the protective role of anthocyanins as "sunscreens" on chlorophylls (Grace & Logan 2000; Feild *et al*. 2001; Nakashima & Yamakita 2023). Given that anthocyanins strongly absorb blue-green light, anthocyanin accumulation may reduce the quality and quantity of light captured by chlorophylls and carotenoids as leaf senescence (Hoch *et al*. 2001; Moustaka *et al*. 2018). This mechanism may protect degrading chloroplasts from photo-inhibition during leaf senescence, give cells the opportunity to re-absorb nutrients before leaf abscission, and slow down the speed of leaf senescence (Ranjan *et al*. 2014; Renner & Zohner 2019).

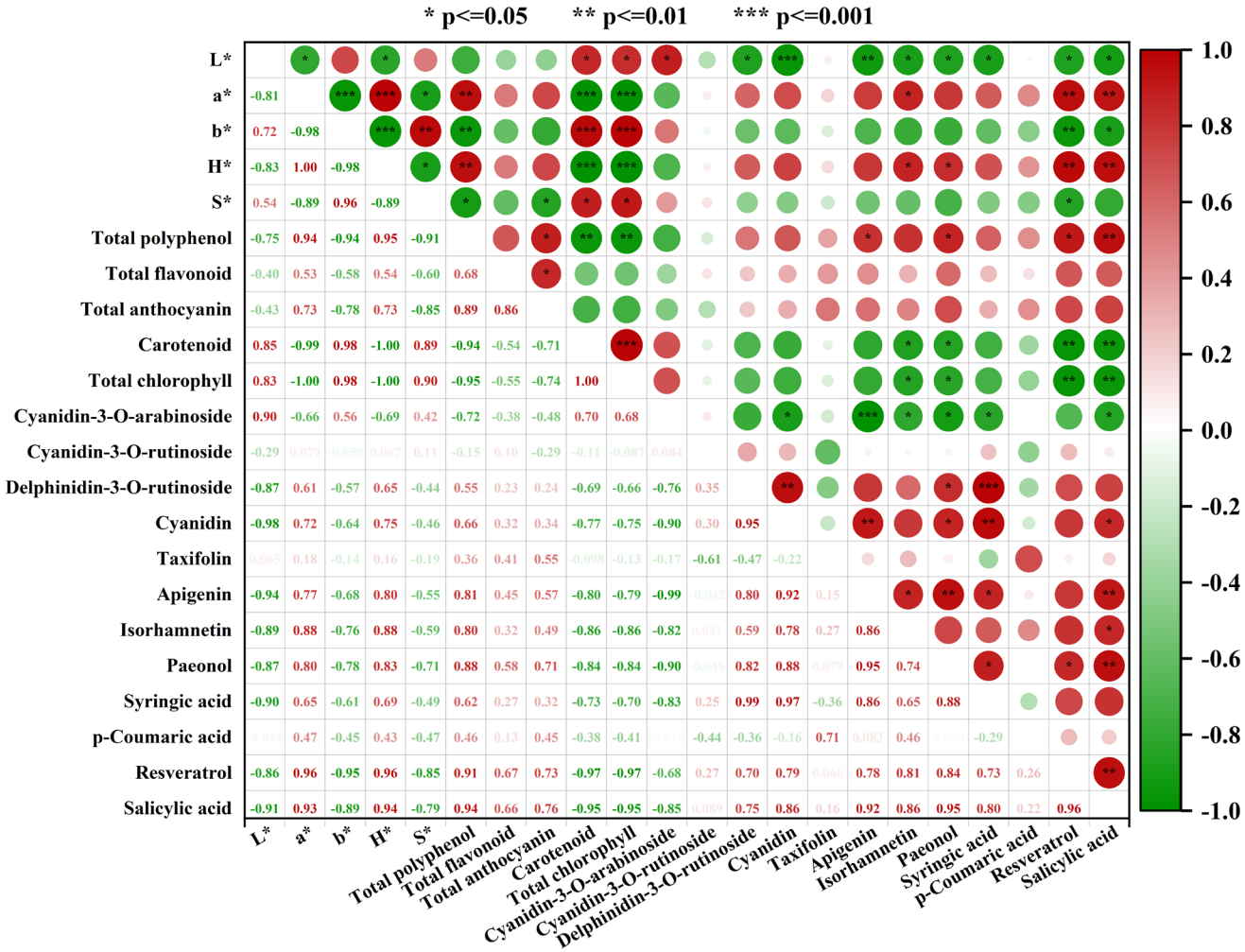

Figure 5. Pearson's correlation analysis between colour values and phenolic metabolites of *Syringa oblata* leaves. Red colour represents positively correlation, green colour represents negatively correlation, and the darker the colour explains the stronger the correlation. * indicates significant correlation at P < 0.05, ** indicates extremely significant correlation at P < 0.01, and *** indicates extremely significant correlation at P < 0.001.

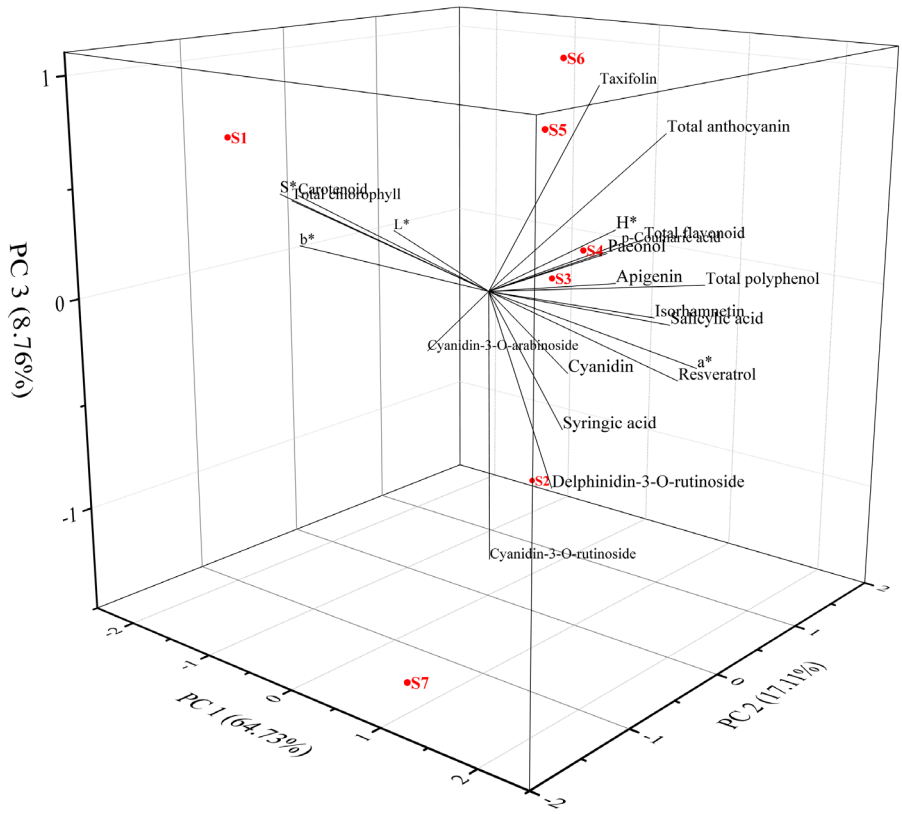

Figure 6. Principal component analysis (PCA) 3D plot. PC1, PC2, and PC3 represent principal component 1, 2, and 3, respectively.

Table 2. The loading plots and coefficients of PCA analysis.

Extracted eigenvectors	Loading plot			Coefficient		
	PC1 (64.73%)	PC2 (17.11%)	PC3 (8.76%)	PC1	PC2	PC3
L*	-1.74	0.53	0.09	-0.24	0.16	0.04
a*	1.73	0.56	-0.27	0.24	0.17	-0.12
b*	-1.74	-0.48	0.13	-0.24	-0.15	0.06
h*	1.64	-0.32	0.45	0.23	-0.10	0.19
S*	-1.11	-1.14	0.49	-0.16	-0.35	0.21
Total polyphenol	1.73	0.63	0.10	0.24	0.19	0.04
Total flavonoid	1.08	0.63	0.26	0.15	0.19	0.11
Total anthocyanin	1.46	0.44	0.77	0.20	0.13	0.33
Total chlorophyll	-1.76	-0.46	0.37	-0.24	-0.17	0.16
Carotenoid	-1.73	-0.55	0.36	-0.25	-0.14	0.15
Cyanidin-3-*O*-arabinoside	-1.55	0.73	-0.54	-0.22	0.22	-0.23
Cyanidin-3-*O*-rutinoside	-0.40	0.40	-1.45	-0.06	0.12	-0.63
Delphinidin-3-*O*-rutinoside	1.48	-0.78	-0.62	0.21	-0.24	-0.27
Cyanidin	1.65	-0.80	-0.10	0.23	-0.24	-0.04
Taxifolin	0.00	1.25	0.85	-1.83E-4	0.38	0.37
Apigenin	1.74	-0.41	0.24	0.24	-0.13	0.10
Isorhamnetin	1.65	0.13	0.01	0.23	0.04	0.00
Paeonol	1.73	-0.50	0.38	0.24	-0.15	0.16
Syringic acid	1.59	-0.78	-0.35	0.22	-0.24	-0.15
p-Coumaric acid	0.04	1.53	0.05	0.01	0.47	0.02
Resveratrol	1.81	0.24	-0.28	0.25	0.07	-0.12
Salicylic acid	1.88	0.05	0.01	0.26	0.01	0.00

Anthocyanins, belonging to polyphenols, are the major pigments helping *S. oblata* leaf colouration. However, there is little research on anthocyanin types in *S. oblata* leaves. Therefore, the anthocyanin types in leaves were evaluated to explore which anthocyanin played the key role on leaf colouration. Delphinidin-3-*O*-rutinoside and cyanidin contents increased as a whole from S1 to S7 and negatively correlated with the L^* value. The results indicated that the changes of cyanidin and delphinidin-3-*O*-rutinoside contents were highly correlated with the phenotypic change of the leaf colour and they are the major anthocyanins contributing to the reddening of leaf. Cyanidin-3-*O*-arabinoside was the most abundant anthocyanin detected in *S. oblata* leaves, and its content decreased slowly with leaf senescence, which may lead to the decrease of total anthocyanin content at S6 and S7. Cyanidin-3-*O*-rutinoside contents were stable during the leaf colouration. Differently, delphinidin-3-*O*-rutinoside and cyanidin-3-*O*-rutinoside were more important than other anthocyanin in purple flowers of *S. oblata*, and changes in their content could influence flower colour change (Ma *et al*. 2022). The ratios of delphinidin glycoside and cyanidin glycoside may influence plant tissue colour, and the ratios were higher in purple tissues than in red ones (Katsumoto *et al*. 2007). This explains that the specific of anthocyanin distributions in different tissues caused the colour difference between leaves and flowers of *S. oblata*.

Anthocyanins are highly water-soluble and are a cationic sub-class of flavonoids, with their precise colour depending on vacuole pH and co-pigmentation processes with other flavonoids, hydroxycinnamic acids or metallic cations (Renner & Zohner 2019; Sun *et al*. 2022; Zhao *et al*. 2022). Among phenolic compounds detected in *S. oblata* leaves, apigenin and syringic acid contents increased with leaf reddening and distinctly positively correlated with delphinidin-3-*O*-rutinoside and cyanidin contents. Supramolecular pigments composed of cyanidins, apigenins and metal ions in a stoichiometric ratio decided cornflower petals colour (Deng *et al*. 2019). A cyanin isolated from *Rosa hybrida* formed a lactone ring with the gallic acid residue (Yoshida *et al*. 2009). These findings suggest that apigenin and syringic acid might be the anthocyanin co-pigments assisting leaf colouration. In addition, abundant phenolic compounds detected in leaves, for example taxifolin, which has extraordinary antioxidant and anti-inflammatory activities (Zhang *et al*. 2021). These results suggest that the leaves of *S. oblata* are a natural source of bioactive substances and inspire the reuse of fallen leaves for economic benefits.

In conclusion, this study demonstrated that leaf reddening of *S. oblata* resulted from anthocyanin accumulation and chlorophyll degradation. During the leaf colouration, the chlorophyll and carotenoid contents evidently decreased. In contrast, the total polyphenol, total flavonoid, and total anthocyanin contents significantly increased, which was consistent with the pigment distribution in leaf cells. Numerous phenolic metabolites were detected in leaves. The key polyphenols that turned leaves red were identified as delphinidin-3-*O*-rutinoside and cyanidin, whose contents significantly correlated with leaf colour values. Moreover, the contents of delphinidin-3-*O*-rutinoside and cyanidin were evidently positively correlated with those of apigenin, paeonol, and syringic acid, which could be the anthocyanins co-pigments.

Acknowledgements

This work was supported by Technological Innovation Programs of Higher Education Institutions in Shanxi Province of China (2021L122), Technological Innovation Programs of Shanxi Agricultural University (2020BQ52) and Fundamental Research Program of Shanxi Province (20210302124687), and Natural Science Foundation of Shanxi Province (202103021224144). We would like to thank TopEdit (https://www.topeditsci.com/) for linguistic assistance during the preparation of this manuscript. Thanks are due to Professor Houhua Li for assistance with the HPLC experiments.

Authors' Contributions

MH: Conception, Investigation, Data curation, Writing original draft, and Funding acquisition; RL: Investigation, Data curation, Writing original draft; MH: Investigation and Data curation; XY: Reviewing original draft and Funding acquisition; FD and XC: Instructing experiment and Reviewing original draft; SH, SL, and DH: Investigation and Collection materials.

Conflict of Interest

The authors report no declarations of interest.

Supplementary material

The following online material is available for this article:

Table S1. The standard curve for phenolic compound contents.

References

Deng C, Wang J, Lu C, Li Y, Hong Y, Dai S. 2019. Metabolite and transcriptome analyses provide new insights into the generation of the blue supramolecular pigment in cornflower. Research Square: 1-24.

Feild TS, Lee DW, Holbrook MN. 2001. Why leaves turn red in autumn: The role of anthocyanins in senescing leaves of red-osier dogwood. Plant Physiology 127: 566-574.

Gao S, Gao J, Zhu X *et al*. 2016. ABF2, ABF3, and ABF4 Promote ABA-Mediated Chlorophyll Degradation and Leaf Senescence by Transcriptional Activation of Chlorophyll Catabolic Genes and Senescence-Associated Genes in *Arabidopsis*. Molecular Plant 9: 1272-1285.

Gazula A, Kleinhenz MD, Streeter JG, Miller AR. 2005. Temperature and Cultivar Effects on Anthocyanin and Chlorophyll b Concentrations in Three Related *Lollo Rosso Lettuce* Cultivars. HortScience 40: 1731-1733.

Grace SC, Logan BA. 2000. Energy dissipation and radical scavenging by the plant phenylpropanoid pathway. Philosophical Transactions of the Royal Society B 355: 1499-1510.

Han J, Zhang J, Yang H *et al*. 2011. Comparative Studies on the flavonoids and polysaccharides from branch of *Syringa* L. *wolfi* schneid. in different harvest. Ginseng Research 4: 24-28.

Han M, Zhao Y, Meng J, Yin J, Li H. 2022. Analysis of physicochemical and antioxidant properties of *Malus* spp. petals reveals factors involved in flower color change and market value. Scientia Horticulturae 310: 111688.

Hoch WA, Zeldin EL, McCown BH. 2001. Physiological significance of anthocyanins during autumnal leaf senescence. Tree Physiology 21: 1-8.

Katsumoto Y, Fukuchi-Mizutani M, Fukui Y *et al*. 2007. Engineering of the rose flavonoid biosynthetic pathway successfully generated blue-hued flowers accumulating delphinidin. Plant & Cell Physiology 48: 1589-1600.

Khusnutdinov E, Sukhareva A, Panfilova M, Mikhaylova E. 2021. Anthocyanin Biosynthesis Genes as Model Genes for Genome Editing in Plants. International Journal of Molecular Sciences 22: 8752.

Lee DW, O'Keefe J, Holbrook NM, Feild TS. 2003. Pigment dynamics and autumn leaf senescence in a New England deciduous forest, eastern USA. Ecological Research 18: 677-694.

Lee JH, Kwon YB, Roh YH *et al*. 2023. Effect of Various LED Light Qualities, Including Wide Red Spectrum-LED, on the Growth and Quality of Mini Red *Romaine Lettuce* (Cv. Breen). Plants 12: 2056.

Li N, Shi J, Wang K. 2014. Profile and antioxidant activity of phenolic extracts from 10 crabapples (*Malus* wild species). Journal of Agricultural and Food Chemistry 62: 574-581.

Li W, Li H, Shi L, Shen P, Li Y. 2022. Leaf color formation mechanisms in *Alternanthera bettzickiana* elucidated by metabolite and transcriptome analyses. Planta 255: 59.

Li W, Yang S, Lu Z *et al*. 2018. Cytological, Physiological, and Transcriptomic Analyses of Golden Leaf Coloration in *Ginkgo Biloba* L. Horticulture Research 5: 12.

Li X, Cai K, Han Z *et al*. 2022. Chromosome-Level Genome Assembly for Acer pseudosieboldianum and Highlights to Mechanisms for Leaf Color and Shape Change. Frontiers in Plant Science 13: 850054.

Li Y, Mao K, Zhao C *et al*. 2012. MdCOP1 ubiquitin E3 ligases interact with MdMYB1 to regulate light-induced anthocyanin biosynthesis and red fruit coloration in apple. Plant Physiology 160: 1011-1022.

Lin B, Ma H, Zhang K, Cui J. 2023. Regulatory mechanisms and metabolic changes of miRNA during leaf color change in the bud mutation branches of Acer pictum subsp. mono. Frontiers in Plant Science 13: 1047452.

Liu Y, Feng X, Zhang Y, Zhou F, Zhu P. 2021. Simultaneous changes in anthocyanin, chlorophyll, and carotenoid contents produce green variegation in pink–leaved ornamental kale. BMC Genomics 22: 455.

Lu Y, Hao S, Liu N, Bu Y, Yang S, Yao Y. 2016. Light affects anthocyanin biosynthesis via transcriptional regulation of cop1 in the ever-red leaves of crabapple M.cv. 'Royalty'. Brazilian Journal of Botany 39: 659-667.

Ma B, Wu J, Shi TL *et al*. 2022. Lilac (*Syringa oblata*) genome provides insights into its evolution and molecular mechanism of petal color change. Communications Biology 5: 2399-3642.

Moustaka J, Panteris E, Adamakis IDS *et al*. 2018. High anthocyanin accumulation in poinsettia leaves is accompanied by thylakoid membrane unstacking, acting as a photoprotective mechanism, to prevent ROS formation. Environmental and Experimental Botany 154: 44-55.

Nakashima S, Yamakita E. 2023. In Situ Visible Spectroscopic Daily Monitoring of Senescence of Japanese Maple (*Acer palmatum*) Leaves. Life 13: 2030.

Nenadis N, Vervoort J, Boeren S, Tsimidou MZ. 2007. *Syringa oblata* Lindl var. *alba* as a source of oleuropein and related compounds. Journal of the Science of Food and Agriculture 87: 160-166.

Ranjan S, Singh R, Singh M, Pathre UV, Shirke PA. 2014. Characterizing photoinhibition and photosynthesis in juvenile-red versus mature-green leaves of Jatropha curcas L. Plant Physiology and Biochemistry 79: 48-59.

Renner SS, Zohner CM. 2019. The occurrence of red and yellow autumn leaves explained by regional differences in insolation and temperature. New Phytologist 224: 1464-1471.

Shen YH, Yang FY, Lu BG *et al*. 2019. Exploring the differential mechanisms of carotenoid biosynthesis in the yellow peel and red flesh of papaya. BMC Genomics 20: 49.

Shi Y, Pang X, Liu W *et al*. 2021. *Sizhd17* is involved in the control of chlorophyll and carotenoid metabolism in tomato fruit. Horticulture Research 8: 259.

Song T, Li K, Wu T *et al*. 2019. Identification of new regulators through transcriptome analysis that regulate anthocyanin biosynthesis in apple leaves at low temperatures. PLoS One 14: e0210672.

Song X, Duan X, Chang X, Xian L, Liu Y. 2021. Molecular and metabolic insights into anthocyanin biosynthesis during leaf coloration in autumn. Environmental and Experimental Botany 190: 104584.

Sui L, Wang K, Liang Y, Xue Q. 2017. The relationships between leaf anatomical structure, anthocyanins and photosynthetic characteristics in Perilla frutescens. Chinese Journal of Ecology 36: 1590-1596.

Sun Q, Guo Y. 2013. Exatraction of total flavononoids from leaves of *Syringa ablata* Lindl. and numerrical simulation. China Journal of Hospital Pharmacy 33: 1145-1149.

Sun X, Shokri S, Gao B *et al*. 2022. Improving effects of three selected co-pigments on fermentation, color stability, and anthocyanins content of blueberry wine. LWT-Food Science and Technology 156: 113070.

Tai B, Bai L, Ji R *et al*. 2022. Phytochemical and pharmacological progress on *Syringa oblata*, a traditional Mongolian medicine. Chinese Herbal Medicines 14: 392-402.

Tang Y, Fang Z, Liu M, Zhao D, Ta J. 2020. Color characteristics, pigment accumulation and biosynthetic analyses of leaf color variation in herbaceous peony (*Paeonia lactiflora* Pall.). 3 Biotech 10: 1-10.

Tian Y, Zhang H, Zhang X, Wang J, Qi F, Sun G. 2014. The relationship between leaf anthocyanin content and chlorophyll fluorescence, as well as excited energy distribution during leaf expansion of *Syringa oblata* Lindl. Journal of Nanjing Forestry University (Natural Sciences Edition) 1: 59-64.

Walibai T, Li H, Li G, Liu T, Li A, Han M. 2017. Pigments Analysis On Different Colors of Leaves from *Malus Sieboldii*. Guihaia 37: 1572-1578.

Wang WB, He XF, Yan XM *et al*. 2023. Chromosome-scale genome assembly and insights into the metabolome and gene regulation of leaf color transition in an important oak species, *Quercus dentata*. New Phytologist 238: 18814.

Wen CH, Lin SS, Chu FH. 2015. Transcriptome Analysis of a Subtropical Deciduous Tree: Autumn Leaf Senescence Gene Expression Profile of Formosan Gum. Plant and Cell Physiology 56: 163-174.

Wolfe K, Wu X, Liu R. 2003. Antioxidant activity of apple peels. Journal of Agricultural and Food Chemistry 51: 609-614.

Xu W, Dubos C, Lepiniec L. 2015. Transcriptional control of flavonoid biosynthesis by MYB–bHLH–WDR complexes. Trends in Plant Science 20: 176-185.

Yoshida K, Mori M, Kondo T. 2009. Blue flower color development by anthocyanins: from chemical structure to cell physiology. Natural Product Reports. 26: 884-915.

Zhang S, Wu X, Cui J *et al*. 2019. Physiological and transcriptomic analysis of yellow leaf coloration in *Populus deltoides* Marsh. PLoS One 14: e0216879.

Zhang X, Lian X, Li H *et al*. 2022. Taxifolin attenuates inflammation via suppressing MAPK signal pathway in vitro and in silico analysis. Chinese Herbal Medicines 14: 554-562.

Zhang ZY, Wang QY, Shi L, Yu WG, Zhang YQ, Cui HX. 2021. Secondary metabolites of *Syringa* and the linking with phylogenetic evolution and geographical distributions. Chinese Bulletin of Botany 56: 470-479.

Zhao X, He F, Zhang XK, Shi Y, Duan CQ. 2022. Impact of three phenolic copigments on the stability and colour evolution of five basic anthocyanins in model wine systems. Food Chemistry 375: 131670.